PCCP

Influence of Gold Additive on the Stability and Phase Transformation of Titanate Nanostructures

Journal:	*Physical Chemistry Chemical Physics*
Manuscript ID:	Draft
Article Type:	Paper
Date Submitted by the Author:	n/a

Complete List of Authors:	Pusztai, Péter; University of Szeged, Department of Applied and Environmental Chemistry Puskás, Róbert; University of Szeged, Department of Applied and Environmental Chemistry Varga, Erika; University of Szeged, Department of Physical Chemistry and Materials Science Erdohely , Andras; University of Szeged, Physical Chemistry and Material Science Kukovecz, Akos; Univ Szeged, Applied & Environmental Chamistry Konya, Zoltan; Univ Szeged, Applied & Environmental Chamistry Kiss, Janos; University of Szeged,

Influence of Gold Additive on the Stability and Phase Transformation of Titanate Nanostructures

P. Pusztai[a], R. Puskás[a], E. Varga[b], A. Erdőhelyi[b], Á. Kukovecz[a,c], Z. Kónya[a,d], J. Kiss[b,d*]

[a]Department of Applied and Environmental Chemistry, University of Szeged, Rerrich Béla tér 1., Hungary, [b]Department of Physical Chemistry and Materials Science, University of Szeged, Aradi vértanuk tere1., H-6720 Szeged, Hungary [c]MTA-SZTE "Lendület" Porous Nanocomposite Research Group, [d]MTA-SZTE Reaction Kinetics and Surface Chemistry Research Group H-6720 Szeged, Rerrich Béla tér 1., Hungary,

*Corresponding author at: Department of Physical Chemistry and Materials Science, University of Szeged, Aradi vértanuk t. 1. H-6720 Szeged, Hungary. fax: +36 62 546482. e-mail: **jkiss@chem.u-szeged.hu**

Abstract

Gold nanoparticles were prepared and characterized on protonated (H-form) titanate nanotubes (TiONT) and nanowires (TiONW). The chemical nature and morphology of gold particles were monitored by X-ray photoelectron spectroscopy (XPS), Raman spectroscopy, X-ray diffraction (XRD) and high resolution electron microscopy (HRTEM). The optical properties of Au-containing titanate nanowires were explored by means of ultraviolet-visible diffuse reflectance spectroscopy. The size distribution and homogeneity of gold particles depends on the reduction mode from the corresponding gold salt to metal particles. Smaller clusters (3-8 nm) were obtained with $NaBH_4$ reactant at 293 K than with molecular hydrogen reduction. An unexpectedly high binding energy gold state was found by XPS in gold-loaded titanate nanostructures. This state was absent from the spectra of gold-loaded TiO_2(110). A likely explanation for this phenomenon, supported also by the characteristic decrease of band gap energy from 3.14 eV to 2.50 eV with increasing Au content, is that the depending on metal loading, Au is stabilized on titanate nanowires partially in positively charged gold form by ion exhange and also as Au clusters. Our important new finding is that the thermal annealing behavior of Au-loaded titanate nanotubes and nanowires is different. The former loose their tubular morphology and are readily transformed into anatase even at the very low temperature of 473 K. On the other hand, gold stabilizes the layered structure of titanate nanowires up to 873 K.

Key words: Key words: titanate nanowire, titanate nanotubes, anatase TiO_2, Au nano particles, XPS, TEM, XRD, titanate Raman spectroscopy

Introduction

One-dimensional TiO_2 related nanomaterials with high morphological specificity, such as nanotubes and nanowires have attracted considerable attention due to their interesting chemical and physicochemical properties.[1-13] Recently a further comprehensive review[14] and article[15] about the fabrication, modification and application of titania nanotubes were published. On the basis of the pioneering work of Kasuga et al.,[16] research efforts on titanates were at first concentrated on the hydrothermal synthesis and structure elucidation of titanate nanotubes. Recently, hydrothermal conversion of self-assembled titanate nanotubes (TiONT) into nanowires (TiONW) in a revolving autoclave was achieved in our laboratory.[17,18] Titanate nanobjects are of great interest for catalytic applications, since their high surface area[15,16] and cation exchange capacity provides the possibility of achieving a high metal (e.g. Co, Cu, Ni, Ag and Au) dispersion.[11,19-21]

Recently it was found that titanate nanostructures (nanowires and nanotubes) can stabilize gold in a very dispersed form.[21,23-30] Up to now some important titanate supported gold catalytic reactions were discovered. Gold-containing titania nanotubes were found to display higher activity than the Degussa P-25 catalyst in the photo-oxidation of acetaldehyde,[25] in the photocatalytic degradation of formic acid,[12] in the water-gas shift reaction[23] and in CO oxidation[23,27-29]. Nanosized gold catalyst on titanate nanowires exhibited excellent efficiency in 4-nitrophenol reduction.[30] There are some examples that other noble metals supported on titanate nanostructures also perform remarkably in catalytic processes. TiO_2 nanofibers decorated either with Pt or Pd nanoparticles show significant photocatalytic behavior as demonstrated by the decomposition of organic dyes in water, the degradation of organic stains on the surface of flexible freestanding cellulose/catalyst composite film and the generation of hydrogen from ethanol using both suspended and immobilized catalysts. The performance of the nanofiber-based catalyst materials competes with their conventional nanoparticle-based counterparts.[31-33] Recently it has been shown that Rh supported on titania nanowires is a better catalyst in the hydrogenation of carbon dioxide than Rh on Degussa P-25 TiO_2 and much better than that on titania nanotubes.[34]

The location of metal ions on the nanocrystal surface may prove important in mediating electron transfer reactions that have relevance in photocatalyis or power storage. Ion exchange allows titanate nanostructures to incorporate metal adatoms in their framework which may create another type of active center besides metal clusters.[10,11,20,21] Studies in this

direction are still scarce in the literature because of the genuine novelty of the titanate nanomaterial based photocatalytic and low-temperature thermal heterogeneous catalysis field. TiO_2 structures are widely used in photochemical applications, whereas titanates offer excellent ion exchange properties,[22] which are absent from rutile and anatase. Therefore, both TiO_2[37] and titanate nanostructures[12,25,31-33] modified by metal nanoparticles are promising materials from the heterogeneous catalytic point of view. Morphology and chemical nature of gold additives on titanate nanotubes and nanowire are the keys to understand the processes driven by gold containing nanomaterials.

Titanate nanotubes are open-ended hollow tubular objects measuring 7-10 nm in outer diameter and 50-170 nm in length. They feature a characteristic spiral cross section composed of 4-6 wall layers. The typical diameter of their inner channel is 5 nm.[16,35] Titanate nanowires represent the thermodynamically most stable form of sodium trititanate under the alkaline hydrothermal conditions applied in titanate nanotube synthesis as well. (Note that the post-synthetic neutralization step converts the original $Na_2Ti_3O_7$ into its hydrogen form without affecting the nanowire morphology.) Their diameter is 45-110 nm and their length is between 1.8 and 5 μm.[17] The specific surface area of titanate nanotubes is rather large (~185 m^2g^{-1}) due to their readily accessible inner channel surface, whereas that of titanate nanowires is ~20 m^2g^{-1}. According to our independent infrared spectroscopic (IR), thermogravimetric and X-ray diffraction (XRD) measurements as well as literature findings[36] the trititanate structure appears to be thermally deconstructed at approx. 573 K. Annealing at higher temperatures initiates the trititanate to anatase conversion process. This phase transformation could be influenced by metal adatoms. Recently we observed Rh-induced transformation phenomena in titanate nanowire and nanotube catalysts.[10] Rh decorated nanowires transform into β-TiO_2 structure, whereas their pristine counterparts' recrystallize into anatase. The formation of anatase was dominant during the thermal annealing process in both acid treated and Rh decorated nanotubes. Transformation to anatase was enhanced in the presence of Rh.[10] These examples also motivated us to study the effect of gold nanoparticles on titanate nanostructures.

In the present work we investigate the chemical nature of gold additives on titanate nanowires and nanotubes by X-ray photoelectron spectroscopy and we study the stability and phase transformation of titanate nanostractures upon gold deposition using Raman spectroscopy, X-ray diffraction (XRD) and transmission electron microscope in high resolution mode (HRTEM).

Experimental

Titanate nanowires and nanotubes were prepared by mixing 2 g of anatase into 140 cm^3 10 M aqueous NaOH solution until a white suspension was obtained, aging the suspension in a closed, cylindrical, Teflon-lined autoclave at 400 K for 1-72 h (depending on the desired product) while rotating the whole autoclave intensively at 60 rpm around its short axis, and finally washing the product with deionized water and neutralizing with 0.1 M HCl acid solution to reach pH=7. At this point, the titanate nanostructures slurry was filtered and dried in air at 353 K.[16,17] Acid washing is a standard method in titanate nanotube and nanowire synthesis. It is used to exchange as much Na^+ ions in the structure to protons as possible. The resulting material is generally referred to as "H-form" titanate. The impurity level of the produced protonated materials was less than 1%. The foreign elements determined by X-ray photoelectron spectroscopy (XPS) were C, Ca, and Na that remained in the product from the preparation process.

Titanate nanostructures were decorated by gold nanoparticles by two methods: (A) the Au containing H-form titanate nanowires and nanotubes samples with the same actual Au loading ($HAuCl_4$), 1-2.5% were obtained by deposition-precipitation method[26,28,29] at pH=7 and at 343 K, followed by treatment in H_2 at 473 K. When the reduction temperature was 573 K, we did not observe any changes in particle sizes and morphology. The second method (B) corresponded to reducing gold with $NaBH_4$. The sodium borohydride reduction of metal ions is a known chemical route to synthesize metal nanoparticles.[38,39] $HAuCl_4$ solution with an appropriate concentration to provide 2.5 wt% gold loading was added to the well-homogenized nanowire or nanotube suspension. After 10 minutes of stirring 50 mg of $NaBH_4$ (separately dissolved in 5 ml of distilled water) was added rapidly to achieve the instantaneous formation of gold nanoparticles at 293 K. The suspension was stirred for further 20 minutes then rinsed with distilled water thoroughly. The as-purified sample was dried overnight in air in a temperature programmed electric oven at 343 K. Quantitative energy-dispersive X-ray spectroscopic (EDX) and XPS analysis showed that after washing the bulk and surface concentration of gold decreased by about 55%. Trace amounts of Na remained in the sample after these post-synthetic treatments. Boron was undetectable in the samples.

XP spectra were taken with a SPECS instrument equipped with a PHOIBOS 150 MCD 9 hemispherical analyzer. The analyzer was operated in the FAT mode with 20 eV pass energy. The Al K_α radiation ($h\nu$=1486.6 eV) of a dual anode X-ray gun was used as an excitation source. The gun was operated at a power of 150 W (12.5 kV, 12 mA). The energy

step was 25 meV, electrons were collected for 100 ms in one channel. Typically five scans were summed to get a single high-resolution spectrum. The Ti $2p_{3/2}$ maximum (458.9 eV) was used as the energy reference. The same data were obtained when C 1s (adventitious carbon at 285.1 eV) or O 1s lattice oxygen (530.4 eV) was used as references. The sample preparation chamber was directly connected to the measuring chamber to avoid the contamination of samples between the steps. For spectrum acquisition and evaluation both manufacturer's (SpecsLab2) and commercial (CasaXPS, Origin) software packages were used.

UV-Vis diffuse reflectance spectra were obtained relative to the reflectance of a standard ($BaSO_4$) using an UV/Vis spectrophotometer (OCEAN OPTICS, Typ.USB 2000) equipped with a diffuse reflectance sampling accessory. The samples were pressed into pellets of 2 g $BaSO_4$ and 50 mg of the titanate material.

Raman spectra of slightly pressed powder samples were measured in 180° backscattered geometry at 785 nm laser excitation (incident laser power 460 mW) using an Ocean Optics QE65000 spectrometer coupled to an Ocean Optics Raman probe. Scans were integrated at 4 cm^{-1} resolution until the desired signal-to-noise ratio of 1000 or better was achieved (typically 30 seconds).

The bulk concentration of the elements was determined by energy-dispersive X-ray spectroscopy (EDX) performed using a Röntec Quantax QX^2 spectrometer built into a Hitachi S-4700 type II cold field emission scanning electron microscope. Spectra were taken at 20 kV acceleration voltage and quantitatively analyzed by the factory standard software after automatic background subtraction and peak fitting.

The morphology of pristine and Au modified titanate nanostructures was characterized by transmission electron microscopy (FEI Tecnai G^2 20 X-Twin; 200 kV operation voltage, x180000 magnification, 125 pm/pixel resolution). X-ray diffractometry (Rigaku MiniFlexII; CuK_α) and electron diffraction technique were used for crystal structure and crystallinity determinations. The Au particle size distribution was determined by image analysis of the HRTEM pictures using the ImageJ software. At least five representative images of equal magnification, taken at different spots of the TEM grid were first subjected to rolling ball background subtraction and contrast enhancement, and then the diameter of the metal nanoparticles in the image was manually measured against the calibrated TEM scale bar. Each diameter distribution histogram was constructed from 200 individual nanoparticle diameter measurements.[10,11]

Results and discussion

1. Preparation and characterization of gold nanoparticles on titanate nanostructures

Atomically dispersed gold can be produced on porous TiO_2 and titania nanostructures (nanotubes, nanowires) by coprecipitation or deposition-precipitation methods.[29,23-25,30] Although it is virtually impossible to prepare a truly monodisperse collection of metallic particles (i.e. particles of exactly the same diameter), in the past years significant progress was made in the preparation of gold particles with a narrow diameter distribution between ~2-10 nm.[23-30,34,40,41] In the present work we produced gold nanoparticles on titanate nanowires and nanotubes in two ways; (A) after deposition-precipitation the reduction step was done with molecular hydrogen at 473 K, or (B) $NaBH_4$ was used for reduction at 293 K (see Experimental). Fig. 1 shows typical HRTEM images obtained with two different reduction procedures on H-form nanowires. In the case of hydrogen reduction (Fig. 1A), the size of Au nanoparticles was mostly between 3.0 and 10.0 nm, but a small fraction was observed at around 15-20 nm as well. A very similar result was obtained on H-form titanate nanotubes. HRTEM and XRD measurements indicated that well-crystallized face-centered cubic gold particles were dispersed on both nanowires and nanotubes. The concentration of the gold precursor slightly affected the gold diameter distribution in the 1-2.5 wt% gold content range. The average size of gold was significantly smaller when the reduction was executed by $NaBH_4$ (Fig. 1B). In this way we obtained a homogeneous distribution: the size of Au nanoparticles was between 3.0 and 8.0 nm on the H-form titanate nanowires. The gold size distribution was very similar on the nanotubes as well, however, a small fraction of the nanoparticles had a diameter of approx. 10 nm.

The chemical environment of the prepared gold nanoparticles was characterized by XPS. The 4f spectra of gold deposited on titanate nanostructures after different reduction procedures and at different gold loading are displayed in Fig. 2. For comparison the figure shows the clean gold film (thickness: 50 nm) prepared on a glass plate. In the 4f region symmetric $4f_{5/2}$ and $4f_{7/2}$ emissions were detected (Fig. 2A). However, the features obtained on titanate nanostructures are quite different (Fig. 2B-D) insofar as two peaks are present in the reduced sample spectra for Au $4f_{7/2}$ at 84.0 eV (metallic state) and at 85.8-86.3 eV.

Two different explanations can be offered for the appearance of this unusually high binding energy gold state. Core level shifts due to particle size must be considered first in the interpretation of the spectra of nanoparticles.[42-44] Although this effect undoubtedly plays a role

in the present case, the observed nearly 2 eV binding energy shift cannot be explained satisfactorily by this way alone. In our previous paper[21] the systematic increase of the binding energy with decreasing cluster size was obvious. The Au $4f_{7/2}$ peak positions were measured as a function of Au coverage. The peak appeared at 84.3 eV at very low coverage (0.04 ML) on the stoichiometric TiO_2(110) surface. The position of this emission shifted slightly to lower binding energy with increasing coverage. Above 1 ML coverage it was located at 84.0 eV, which corresponds to the bulk position. The observed shift can be attributed to the finite size of the clusters combined with the insulating nature of the substrate, which results in a less efficient screening of the core hole formed in the photoemission process. On reduced TiO_2(110) the binding energy shift from submonolayer to monolayer is larger (>0.6 eV) than that on the stoichiometric surface as indicated by the Au $4f_{7/2}$ spectra recorded at different gold coverages. It was shown experimentally that increasing the number of surface defects could enhance the nucleation probability. The deposited Au forms smaller size crystallites in higher density on thermally reduced or Ar^+ ion sputtered surfaces relative to the stoichiometric substrate.[44,45] Although this effect certainly plays a role in the present case as well, since titanate nanowires and nanotubes obviously contain a large number of defects and irregularities, the observed nearly 2 eV binding energy shift cannot be explained satisfactorily by this way alone. The second possible explanation is that Au may have undergone an ion exchange process. This is not possible on TiO_2(110) because of the lack of cations compensating the framework charge, however, it is quite likely to happen on titanates which are well-known for their ion-exchange ability.[22] The cationic character of gold (Au^+) represents a higher binding energy position in our XPS compared to metallic gold state. When Au deposited as Au^+ ions at 1 eV impact energy on rutile TiO_2 samples was studied by XPS,[46] a high binding energy state at 85.8 eV was also observed, which further supports our explanation. Moreover, XPS showed partially charged Au^+ species with binding energy of 84.3-84.6 eV by deposition on nanoceria at low coverages.[47] It was shown that nanoceria stabilizes small Au clusters, which may even be incorporated into ceria nanoparticles.

It can be seen in Fig. 2 that the relative intensity of the higher binding energy peak is larger at 1 wt% gold loading that at 2.5 wt% content (Fig. 2B-C). This means that at lower loading relatively more gold atoms can occupy ion exchange positions (86.1-86.3 eV). It is remarkable that at the same loading relatively less gold occupies the ion exchange position after reduction with $NaBH_4$ (Fig. 2D). It is very likely that the strong reducing agent reduces the positively charged gold from the ion exchange positions to metallic states during the reaction.

An XPS-independent proof for the ion exchange can be obtained by measuring the band gap energy. Cheng et al. have provided theoretical evidence for ion exchange induced band gap reduction in a similar system (Ni-manganite).[48] In our experimental work the band gap energy (E_g) was calculated according to Beranek and Kisch[49] who used the equation $\alpha = A(h\nu - E_g)^n / h\nu$, where α is the absorption coefficient, A is a constant, $h\nu$ is the energy of light and n is a constant depending on the nature of the electron transition. Assuming an indirect band gap (n = 2) for TiO_2[50] with α proportional to $F(R_\infty)$, the band gap energy can be obtained from Kubelka-Munk plots (not shown) of $[F(R_\infty)/ h\nu]^{1/2}$ vs. $h\nu$ as the interception at $[F(R_\infty)/ h\nu]^{1/2} = 0$ of the extrapolated linear part of the plot. The band gap for pure titanate nanowires and nanotubes was 3.14 eV, while that for Au-doped titanate nanowire was less: 2.84 eV at 1 wt% and 2.50 eV at 2.5 wt% Au content. Somewhat smaller decreases in band gap energy were measured for gold containing nanotubes (2.81 eV at 2.50 wt% Au content). When the gold was reduced by $NaBH_4$ at 293 K, these values were 2.74 eV and 2.83 eV for nanowires and nanotubes, respectively. The pronounced decrease of the band gap of titanate nanostructures upon loading with Au suggests a very strong electronic interaction between the titanate nanostructure framework and gold, which may eventually result in an ion exchange process similar to that occurring in silver and cobalt loaded titanates.[11,20] In our previous study[20] it was observed that the band gap decreased from 3.14 eV to 2.41 eV with increasing Co content up to 2 wt% cobalt content. This drastic reduction was not observed when Co was deposited in a similar way on commercial TiO_2. Recently a facile method was also developed to attach transition metal ions (Cr^{3+}, Mn^{2+}, Fe^{2+}, Co^{2+}, Ni^{2+} and Cu^{2+}) to the surface of anatase TiO_2 nanorods.[51]

We may conclude that the higher binding energy XPS peak (85.8-86.4 eV) is due primarily to gold located in cation positions and – to a lesser extent – to gold clusters which are in well-dispersed form. The ratio of these two components depends on the metal content and the preparation method. Remarkable conclusions can be drawn from the XPS intensity changes during heat treatment (Fig. 3). When the gold containing nanowires (2.5%) were treated at 473 K and at 673 K in vacuum for 60 min, the higher binding energy peak remained at 86.4 eV, however, its intensity decreased only slightly (Fig. 3A). This means that the heat treatment did not induce any significant gold segregation from ion exchange position. Interestingly, at same metal loading lower Au 4f XPS intensities were measured in the case of nanotubes (Fig. 3B). It is very likely that a significant part of gold clusters occupy appropriate positions in the inner channel of the tube instead of the outer nanotube shell. A rough semi-quantitative XPS analysis indicates that nearly 75 % of the gold could be located in the inside

of the tube. Further intensity changes (50 %) were measured above 473 K heat treatment. This change is most likely due to further gold penetration into the tube as well as to the morphological transformation of the tube structure induced by gold adatoms (see below).

2. Phase stability and phase transformation of titanate nanostructues upon gold loading

Raman spectra of acid washed H-form titanate nanotubes and nanowires are presented in Fig. 4A and 4B together with the spectrum of a reference anatase sample. The spectra of synthesized nanostructures match previous trititanate results where peaks in the 400-1000 cm^{-1} region were assigned to Ti-O-Ti stretching vibrations.[52,53] The thermal behavior of the samples basically confirms our independent thermogravimetric and XRD measurements as well as literature findings[53] insofar as the trititanate structure appears to be deconstructed at around 673 K (Fig. 4A). Peaks at 393, 514 and 636 cm^{-1} are assigned to the B_{1g}, A_{1g}, and E_{2g} modes of anatase, respectively.[52] A characteristic difference between the behavior of titanate nantubes and nanowires is that in heat treated nanotubes the E_{2g} mode is found at exactly the anatase position (636 cm^{-1}) from 573 K onward, whereas in nanowires this mode experiences a gradual red shift from 648 cm^{-1} at 573 K to 636 cm^{-1} at 873 K (Fig. 4B). A similar effect was observed by Du et al.[54] and Scepanovic et al.[55] in their in situ temperature-dependent Raman studies of nanocrystalline anatase. They argued that defects and nonstoichiometric composition could have a pronounced effect on the position of the soft E_g modes. Adopting this argument to one-dimensional trititanates suggests that the thin and hollow structure of nanotubes is more easily converted to defect-free anatase than the bulky nanowires.

Figures 4C presents the Raman spectra of 2.5 wt% Au loaded titanate nanotubes as a function of heat treatment temperature. The transformation of Au loaded nanotubes features to anatase features starts immediately with the heat treatment. The characteristic anatase peaks at 393, 514 and 636 cm^{-1} (assigned to the B_{1g}, A_{1g} and E_{2g} modes, respectively) appeared already at 473 K. This shows that gold catalyses the transformation of the tube structure to anatase. It seems that this catalytic ability of Au is somewhat higher than that of Rh under the same experimental conditions. In the case of Rh adatoms a clear anatase phase could be identified at 673 K in the Raman spectra.[10]

A markedly different Raman spectral feature was observed in the case of Au loaded titanate nanowires (Fig. 4D). The spectra taken at different temperatures preserved the features corresponding to the wire-like structure with some spectral bordering. Moreover,

there were no sign of anatase structure formation. These Raman results are consistent with our independent XRD and HRTEM measurements.

For comparison the structure and thermal behavior of gold-free titanate nanostructures were also studied in present work by X-ray diffraction. As XRD patterns show (Fig. 5A), the acidic treatment resulted in the degradation of the initial crystal structure of titanate nanotubes, which manifested in the disappearance of the reflection characteristic of the tubular interlayer distance ($2\Theta = \sim 10°$). Protonation also induced the transformation of the titanate nanostructure to anatase form.[10] Thermal treatment below 673 K had no significant effect on the crystal structure; however, at elevated temperature the anatase formation became relevant as evidenced by the appearance of the anatase reflections. The formation of anatase dominated the thermal annealing process from 673 K as indicated by the appearance of anatase reflections (101), (004), (200), (105), (211) and (204) at 25.3°, 37.8°, 48.1°, 53.9°, 55.1° and 62.4°, respectively.

When the H-form titanate nanotubes were decorated with 2.5 wt% gold adatom, anatase reflections appeared already at 473 K indicating that the transformation from the trititanate to anatase is very advantageous (Fig. 5B). For comparison it is worth mentioning that gold is a better catalyst for this transformation than rhodium.[10] Moreover, the presence of sodium retards the transformation of titanate into TiO_2, thus shifting the formation of anatase phase to higher temperatures.[12] When the gold decoration procedure (reduction with hydrogen) resulted in some larger crystallites, extra reflexions due to gold were also detected. In Fig. 5B the gold reflexions are marked at 38.2^0 (1 1 1), 44.4^0 (2 0 0), 62.5^0 (2 2 0) and 77.5^0 (3 1 1).

H_2O washed pristine nanowires feature a mixture of different crystalline titanate forms, mostly β-TiO_2 and $H_xNa_{(2-x)}Ti_3O_7$ as shown in the XRD patterns (Fig. 6A). The β-TiO_2 phase was identified on the basis of its reflections with Miller indices of (2 0 0), (1 1 0), (0 0 2), (1 1 1), (0 0 3), (0 2 0), (0 2 2), (7 1 $\underline{1}$), (3 1 3), (0 2 3) and (7 1 2) at 15.4°, 24.9°, 28.6°, 29.4°, 43.5°, 48.5°, 57.3°, 58.3°, 61.7°, 68.2° and 76.8°, respectively. The $H_xNa_{(2-x)}Ti_3O_7$ phase was identified on the basis of its reflections with Miller indices of (0 0 1), (1 0 1), (0 1 1), (3 0 0), ($\underline{2}$ 0 3) and (4 0 1) found at 10.5°, 15.8°, 25.7°, 29.9°, 34.2° and 43.9°, respectively. Acidic treatment (H-form) also resulted in crystallinity degradation. The crystal transformation is continuous during the thermal annealing process. XRD patterns recorded from a sample annealed at 473 K and 573 K indicated the collapse of the layered structure and the appearance of an anatase phase with low crystallinity. At higher temperatures the formation of the anatase phase becomes dominant as demonstrated by the

appearance of the characteristic anatase reflections (1 0 1), (0 0 4), (2 0 0), (1 0 5), (2 1 1) and (2 0 4) at 25.3°, 37.8°, 48.1°, 53.9°, 55.1° and 62.4°. The process is accompanied by the loss of peak intensities at positions corresponding to the titanate interlayer distance (~10°) β-titanate structural reflections (1 0 1) at 15.8° and (3 0 0) at 29.9°.

The nanowires preserve the wire-like morphology during the heat treatment up to 873 K. However, more and more textural discontinuities can be observed at higher temperatures. The holey structure can be attributed to the continuous transformation of protonated titanate nanostructures to TiO_2 (anatase) followed by water formation and release from the structure. This processes results in the rearrangement of the anatase crystals and the appearance of voids in the structure of the nanowire (Figure 6A).

The XRD profiles of gold decorated nanowires are shown in Fig. 6B as a function of heat treatment. The most important result is that unlike in titanate nanotube, gold did not cause any phase transformations in titanate nanowires. Neither anatase phase formation nor β-TiO_2 structure development were detected by XRD. The visible reflections can all be assigned to gold particles: 38.2° (1 1 1), 44.4° (2 0 0), 64.5^0 (2 2 0) and 77.5^0 (3 1 1). It is worth noting that the effect of gold adatoms on the structure and stability of titanate nanowires is significantly different from those of Rh. In our previous studies it was demonstrated that Rh induces the transformation of the wire structure to β-TiO_2 above 573 K.[10]

TEM images demonstrate the tubular morphology of the as-synthesized titanate nanotubes with a diameter of ~7 nm and length up to 80 nm (not shown here). The acid washing process resulted in a mild destruction of the inner and outer nanotube walls (Fig. 7A). In agreement with the XRD results no morphological degradation could be observed after heat treatment up to 573 K. At higher temperatures the tubular structure started to collapse and transform into rod-like nanostructures (Fig. 7A). At 873 K the tubular morphology totally collapsed that resulted in short nanorods and TiO_2 nanoparticles with an average diameter of ~10 nm. However, when the titanate nanotubes were decorated with gold, the tube structure was destroyed as low as at 473 K. The HRTEM images are presented from 473 K in Fig. 8B-D in two resolutions; in 100 nm and 20 nm, respectively. For comparison H-form titanate nanotubes without gold are also displayed in Fig. 8A. The morphology did not change any further up to 878 K. These HRTEM results agree well with our Raman and XRD findings (Fig. 4 and Fig. 5) and confirm that the gold additive promotes the development of anatase phases.

The titanate nanowire TEM results presented in Fig. 7B confirm that the wire-like morphology is preserved up to 873 K during heat treatment, and they also provide morphological evidence to support the hypothesis presented above about water loss being responsible for the appearance of textural discontinuities.

HRTEM images of gold-decorated H-form titanate nanowires subjected to annealing at different temperatures are shown in two resolutions (100 nm and 20 nm) in Fig. 9B-D. A characteristic image of pristine H-form titanate nanowires is also presented in Fig. 9A as reference. In agreement with the XRD results, the HRTEM images have confirmed that the nanowires preserve their wire-like morphology up to 873 K. Our important new finding is that the thermal annealing behavior of Au loaded titanate nanotubes and nanowires is different. The former lose their tubular morphology and are readily transformed into anatase even at the very low temperature of 473 K. On the other hand, gold stabilizes the layered structure of titanate nanowires up to 873 K. The morphology stabilization effect of gold was independent from the method used for its reduction. HRTEM results displayes in Fig. 10 show that the wire-like morphology is stable with the temperature even the gold nanoparticles were prepared by $NaBH_4$ reactant. It seems that the effect gold is different from that of rhodium[10] as Rh-decorated nanowires have been shown to transform into β-TiO_2 earlier.

Conclusions

Au nanoparticles were prepared and characterized on protonated (H-form) titanate nanotubes and nanowires. The chemical nature and morphology of gold particles were monitored by XPS, Raman spectroscopy, XRD and HRTEM. The optical properties of Au-containing titanate nanowires were explored by ultraviolet-visible diffuse reflectance spectroscopy.

1. The size distribution and homogeneity of gold particles depend on the method used for reducing the dissolved gold salt into deposited nanoparticles. Smaller clusters (3-8 nm) were obtained with $NaBH_4$ reactant at 293 K than with molecular hydrogen reduction at 473 K.

2. An unexpectedly high binding energy gold state was found by XPS in gold-loaded titanate nanostructures. This state was absent from the spectra of gold-loaded TiO_2(110) and gold thick film prepared on glass. A likely explanation for this phenomenon is that the depending on metal loading, Au is stabilized on titanate nanowires partially in positively charged gold form by ion exhange and also as Au clusters. This hypothesis is further

supported by the characteristic decrease of band gap energy from 3.14 eV to 2.50 eV with increasing Au content.

3. Our important new finding is that the thermal annealing behavior of Au loaded titanate nanotubes and nanowires is different. The former loose their tubular morphology and are readily transformed into anatase even at the very low temperature of 473 K. On the other hand, gold stabilizes the layered structure of titanate nanowires up to 873 K. Without gold adatoms the pristine titanate nanowires transform into anatase above 673 K. All these morphological changes – caused either by heat treatment or by a metal induced phase transformation – should be considered in the interpretation of certain catalytic reaction mechanisms or other physical chemical processes conducted on titanate nanostructures. It seems that gold adatoms have the ability to stabilize the wire-like morphology of nanostructured trititanates.

Acknowledgements

The financial support of the TÁMOP-4.2.2.A-11/1/KONV-2012-0047, TÁMOP-4.2.2.A-11/1/KONV-2012-0060 and the Hungarian Scientific Research Fund OTKA NN 110676 is acknowledged. The authors thank gratefully the preparation of the Au decorated titanate nanocomposites to Mrs. Kornélia Baán and the XRD measurements to Mr. László Nagy.

References:

1 D.V. Bavykin, J.M. Friedrich, F.C. Walsh, *Advanced Mater.,* 2006, **18,** 2807‑2824.

2 M. Hodos, E. Horváth, H. Haspel, Á. Kukovecz, Z. Kónya, I. Kiricsi, *Chem. Phys. Lett.,* 2004, **399,** 512-515.

3 G.K. Mor, K. Shankar, M. Paulose, O.K. Varghese, C.A. Grimes, *Nano Lett.,* 2005, **5,** 191-195.

4 S. Kubota, K. Johkura, K. Asanuma, Y. Okouchi, N. Ogiwara, K. Sasaki, T. Kasuga, *J. Mater. Sci.: Mater. Med.,* 2004, **15,** 1031-1035.

5 L. Kavan, M. Kalbac, M. Zukalova, I. Exnar, V. Lorenzen, R. Nesper, M. Graetzel, *Chem. Mater.,* 2004, **16,** 477-485.

6 D. Bavykin, A.A. Lapkin, P.K. Plucinski, J.M. Friderich, F.C. Walsh, *J. Phys. Chem. B,* 2005, **109,** 19422-19427.

7 R. Huang, F. Chung, E.M. Kelder, *J. Electrochem. Soc.,* 2006, **153,** A1459-A1465.

8 R. Dominko, E. Baudrin, P. Umek, D. Arcon, M. Gaberscek, M. Jamnik, *J. Electrochem. Commun.,* 2006, **8,** 673-677.

9 M.T. Byrne, J.M. McCarty, M. Bent, R. Blake, Y.K. Gun'ko, E. Horváth, Z. Kónya, Á. Kukovecz, I. Kiricsi, J.N. Coleman, *J. Mater. Chem.,* 2007, **17,** 2351-2358.

10 G. Pótári, D. Madarász, L. Nagy, B. László, A. Sápi, A. Oszkó, Á. Kukovecz, A. Erdőhelyi, Z. Kónya, J. Kiss, *Langmuir,* 2013, **29,** 3061-3072.

11 D. Madarász, G. Pótári, A. Sápi, B. László, C. Csudai, A. Oszkó, Á. Kukovecz, A. Erdőhelyi, Z. Kónya, J. Kiss, J. *Phys. Chem. Chem. Phys.,* 2013, **15,** 15917-15925.

12 A. Turki, H. Kochkar, C. Guillard, G. Berhault, A. Ghorbel, *Appl. Catal. B: Environmental,* 2013, **138-139,** 401-415.

13 P. Yang, D.K. Zhong, M. Yuan, A.H. Rice, D.R. Gamelin, C.K. Luscombe, *Phys. Chem. Chem. Phys*., 2013, **15,** 4566-4572.

14 H.-H Ou, S.-L. Lo, *Separ. Purif. Technol.,* **2007,** 58, 179-191.

15 L. Torrente-Murciano, A.A. Lapkin, D. Chadwick, *J. Mater. Chem.,* 2010, **20,** 6484-6489.

16 T. Kasuga, M. Hiramatsu, A. Hoson, T. Sekino, *Langmuir,* 1998, **14,** 3160-3163.

17 E. Horváth, Á. Kukovecz, Z. Kónya, I. Kiricsi, *Chem. Mater.,* 2007, **19,** 927-931.

18 Á. Kukovecz, M. Hodos, E. Horváth, G. Radnóczi, Z. Kónya, I. Kiricsi, *J. Phys. Chem. B,* 2005, **109,** 17781-17783.

19 X. Sun, Y. Li, *Chem. Eur. J*., 2003, **9,** 2229-2238.

20 F. Cesano, S. Bertarione, M.J. Uddin, G. Agostini, D. Scarano, A. Zeccina, *J. Phys. Chem. C,* 2010, **114,** 169-178.

21 J. Kiss, P. Pusztai, L. Óvári, K. Baán, G. Merza, A. Erdőhelyi, Á. Kukovecz, Z. Kónya, *eJ. Surf. Sci. and Nanotechnol.* 2014, **12,** 252-258.

22 D. Madarász, I. Szenti, A. Sápi, J. Halász, Á. Kukovecz, Z. Kónya, *Chem. Phys. Lett.,* 2014, **591,** 161-165.

23 T. Akita, M. Okumura, K. Tanaka, K. Ohkuma, M. Kohyama, T. Koyanagi, M. Data, S. Tsubota, M. Haruta, *Surf. and Interf. Anal.,* 2005, **37,** 265-269.

24 V. Idakiev, Z. Yuan, T. Tabakova, B.L. Su, *Appl. Catal. A: General,* 2005, **281,** 149-155.

25 S.S. Malwadkar, R.S. Gholap, S.V. Awante, P.V. Korake, M.G. Chaskar, N.M. Gupta, *N.M. Photochem. Photobiol. A: Chem.,* 2009, **203,** 24-31.

26 Á. Kukovecz, G. Pótári, A. Oszkó, Z. Kónya, A. Erdőhelyi, J. Kiss, *Surf. Sci.,* 2011, **605,** 1048-1055.

27 M. Mendez-Cruz, J. Ramirez-Solis, R. Zanella, *Catal. Today,* 2011, **166,** 172-179.

28 S. Tsubota, M. Haruta, T. Kobayashi, A. Ueda, A.; Nakahara, in: *G. Poncelet et al., Eds., Preparation of Catalysts V, Elsevier Science* B.V. 1991, pp. 695-704.

29 M. Haruta, *Catal. Today,* 1997, **36,** 153-166.

30 G. Chen, F. Xue, Z. Chen, X. Si, X Zheng, J. Huang, S. Massey, *NANO,* 2014, **9,** 1450039-1450046.

31 M-C. Wu, A. Sápi, A. Avila, M. Szabó, J. Hiltunen, G. Tóth, Á. Kukovecz, Z. Kónya, R. Keiski, W-F. Su, H. Jantunen, K. Kordás, *Nano Research,* 2011, **4,** 360-369.

32 M-C. Wu, J. Hiltunen, A. Sápi, A. Avila, W. Larsson, H.-C. Liao, M. Huuhtanen, G. Tóth, A. Shchukarev, N. Laufer, Á. Kukovecz, Z. Kónya, J.-P. Mikkola, R. Keiski, W.-F.Chen, H. Jantunen, P.M. Ajayan, R. Vajtai, K. Kordas, *ACS Nano, 2010*, **5,** 5025-5030.

33 M.C. Wu, G. Tóth, A. Sápi, A. Leino, Z. Kónya, Á. Kukovecz, W.F. Su, K. Kordás, J. *Nanosci. Nanotech.,* 2012, **12,** 1421-1424.

34 M. Tóth, J. Kiss, A. Oszkó, G. Pótári, B. László, A. Erdőhelyi, *Topics in Catal.,* 2012**, 55,** 747-756.

35 S. Zhang, T. Y. Peng, Q. Chen, G. H. Du, G. Dawson and W. Zhou, *Phys. Rev. Lett.,* 2003 **91,** 256103-256105.

36 T. Ohsaka, F. Izumi and Y. Fujiki, *J. Raman Spec.,* 1978**, 7,** 321-325.

37 M. A Henderson, *Surf. Sci. Rep*., 2011, **66,** 185-297.

38 G. N. Glavee, K.J. Klabunde, C.M. Sorensen, G.C. Hadjipanayis, *Inorganic Chem.,* 1995, **34,** 28-35.

39 E.A. Sterling, J. Stolk, L. Hafford, M. Gross, *Metallurgical and Materials Trans.,* 2009, **40A,** 1701-1709.

40 F. Boccuzzi, A. Chiorino, M. Manzoli, P. Lu, T. Akita, S. Ichikawa, M. Haruta, *J. Catal.,* 2001, **202,** 256-267.

41 J. Kiss, L. Óvári, A. Oszkó, G. Pótári, M. Tóth, K. Baán, A. Erdőhelyi, *Catal. Today,* 2012, **181,** 163-170.

42 C.R. Henry, *Surf. Sci. Rep.,* 1988, **31,** 231-233, 235-325.

43 S. Peters, S. Peredkov, M. Neeb, W. Eberhardt, M. Al-Hada, *Surf. Sci.,* 2013, **608,** 129-134.

44 B.K. Min, W.T. Wallace, D.W. Goodman, *Surf. Sci.,* 2006, **600,** L7-L11.

45 A.M. Kiss, M. Svec, A. Berkó, *Surf. Sci.,* 2006, **600,** 3352-3360.

46 C. Fan, T. Wu, S.L. Anderson, Surf. Sci., 2005, **578,** 5-19.

47 M. Baron, O. Bondarchuk, D. Stacchiola, S. Shaikhutdinov, H.-J. Freund, *J. Phys. Chem. C,* 2008, **113,** 6042-6049.

48 J.R. Huang, H. Hsu, C. Cheng, *J. Magnetism and Magnetic Materials,* 2014, **358-359,** 149-152.

49 R. Beranek and H. Kisch, *Photochem. Photobiol. Sci.,* 2008, **7,** 40-48.

50 H. Tang, K. Prasad, R. Sanilines, P. E. Schmid, F. Lewy, *J. Appl. Phys.,* 1994, **75,** 2042-2047.

51 C. Balasanthiran, J.D. Hoefelmeyer, *Chem. Commun.,* 2014, **50,** 5721-5724.

52 R. Ma, K. Fukuda, T. Sasaki, M. Osada, Y. Bando, *J. Phys. Chem. B,* 2005, **109,** 6210-6214.

53 T. Oshaka, F. Izumi, Y. Fujiki, *J. Raman Spectrosc.,* 1978, **7,** 321-324.

54 Y.L. Du, Y. Deng, M.S. Zhang, *J. Phys. Chem. Solids,* 2006, **67,** 2405-2408.

55 M.J. Scepanovic, M. Grujic-Brojcin, Z.D. Dohcevic-Mitrovic, Z.V. Popovic, *Sci. Sintering,* 2009, **41,** 67-73.

Legend of Figures

Fig. 1. HRTEM image on Au decorated H-form titanate nanowires obtained with H_2 reduction (A) and obtained with $NaBH_4$ reduction (B). The corresponding particle size distributions are also shown. The gold contents were 2.5 wt% in both cases.

Fig. 2. Au 4f XPS on differentially prepared Au/titanate samples: (A) clean Au film, (B) 1 wt% Au/titanate nanowire obtained by H_2 reduction at 473 K, (C) 2.5 wt% Au/titanate nanowire obtained by H_2 reduction at 473 K, (D) 2.5% Au/titanate nanowire obtained by $NaBH_4$ reduction at 293 K.

Fig. 3. Au 4f XPS on Au loaded H-form titanate nanowires (A) and nanotubes (B) at 2.5 wt% gold content after heat treatment in vacuum for 60 min.

Fig. 4. Normalized Raman spectra of the thermal behavior of H-form titanate nanotubes (A) and nanowires (B). Graphs C and D illustrate the thermal behavior of Au loaded titanate nanotubes and wires, respectively. The commercial anatase reference sample is shown at the top of each spectra.

Fig. 5. XRD of H_2O washed and H-form titanate nanotubes (upper part) and Au loaded (2.5%) nanotubes (lower part) as a function of annealing temperature.

Fig. 6. XRD of H_2O washed and H-form titanate nanowires (upper part) and Au loaded (2.5%) nanowires (lower part) as a function of annealing temperature.

Fig. 7. TEM images of H-form nanotubes (A) and H-form nanowires (B) at different temperatures.

Fig. 8. HRTEM images of H-form titanate nanotubes (A) and Au containing (2.5 %) nanotubes after different heat treatments; B – 473 K, C – 673 K, D – 873 K.

Fig. 9. HRTEM images of H-form titanate nanowires (A) and Au containing (2.5 %) nanowires after different heat treatments; B – 473 K, C – 673 K, D – 873 K.

Fig. 10. HRTEM images of Au containing (2.5 %) nanowires (obtained by $NaBH_4$ reduction). H-form titanate nanowires (A) and after different heat treatments; B – 473 K, C – 673 K, D – 873 K.

Highlights

Au is stabilized on titanate nanowires partially in positively charged gold form and also as Au clusters. Au loaded nanotubes loose their tubular morphology and are readily transformed into anatase. On the other hand, gold stabilizes the layered structure of titanate nanowires.

ToC

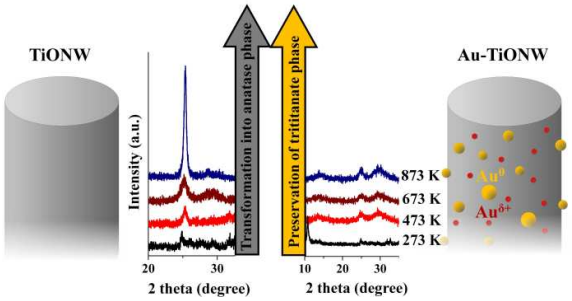

ToC

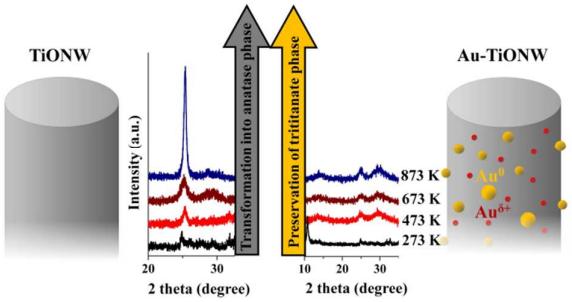
TiONW
Au-TiONW
Intensity (a.u.)
Transformation into anatase phase
Preservation of trititanate phase
873 K
673 K
473 K
273 K
Au0
Auδ+
20
30
2 theta (degree)
10
20
30
2 theta (degree)

Figure 1

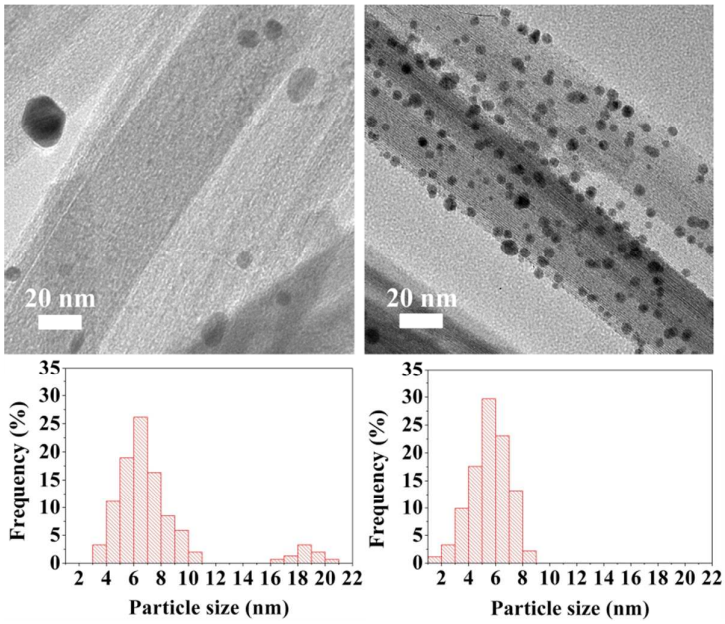

Fig. 1. HRTEM image on Au decorated H-form titanate nanowires obtained with H_2 reduction (A) and obtained with $NaBH_4$ reduction (B). The corresponding particle size distributions are also shown. The gold contents were 2.5 wt% in both cases.

Figure 2

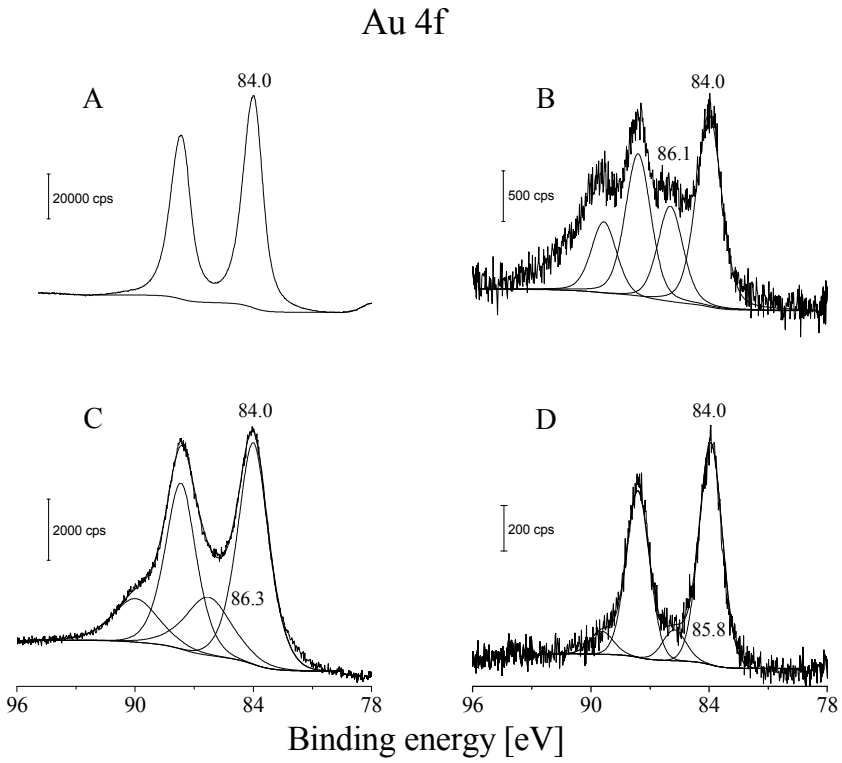

Fig. 2 Au 4f XPS on differentially prepared Au/titanate samples: (A) clean Au film, (B) 1 wt% Au/titanate nanowire obtained by H_2 reduction at 473 K, (C) 2.5 wt% Au/titanate nanowire obtained by H_2 reduction at 473 K, (D) 2.5% Au/titanate nanowire obtained by $NaBH_4$ reduction at 293 K.

Figure 3

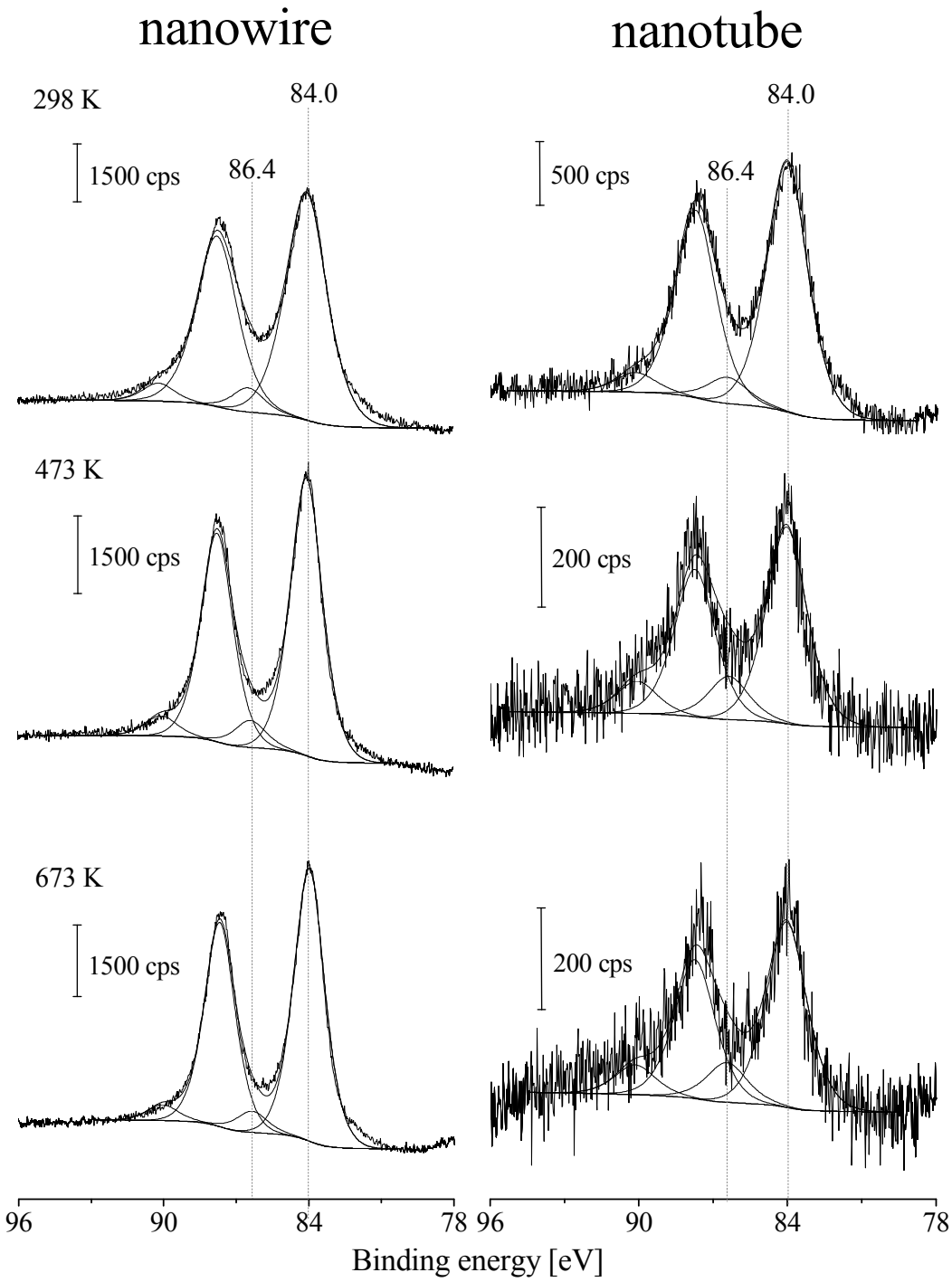

Fig. 3. Au 4f XPS on Au loaded H-form titanate nanowires (A) and nanotubes (B) at 2.5 wt% gold content after heat treatment in vacuum for 60 min.

Figure 4

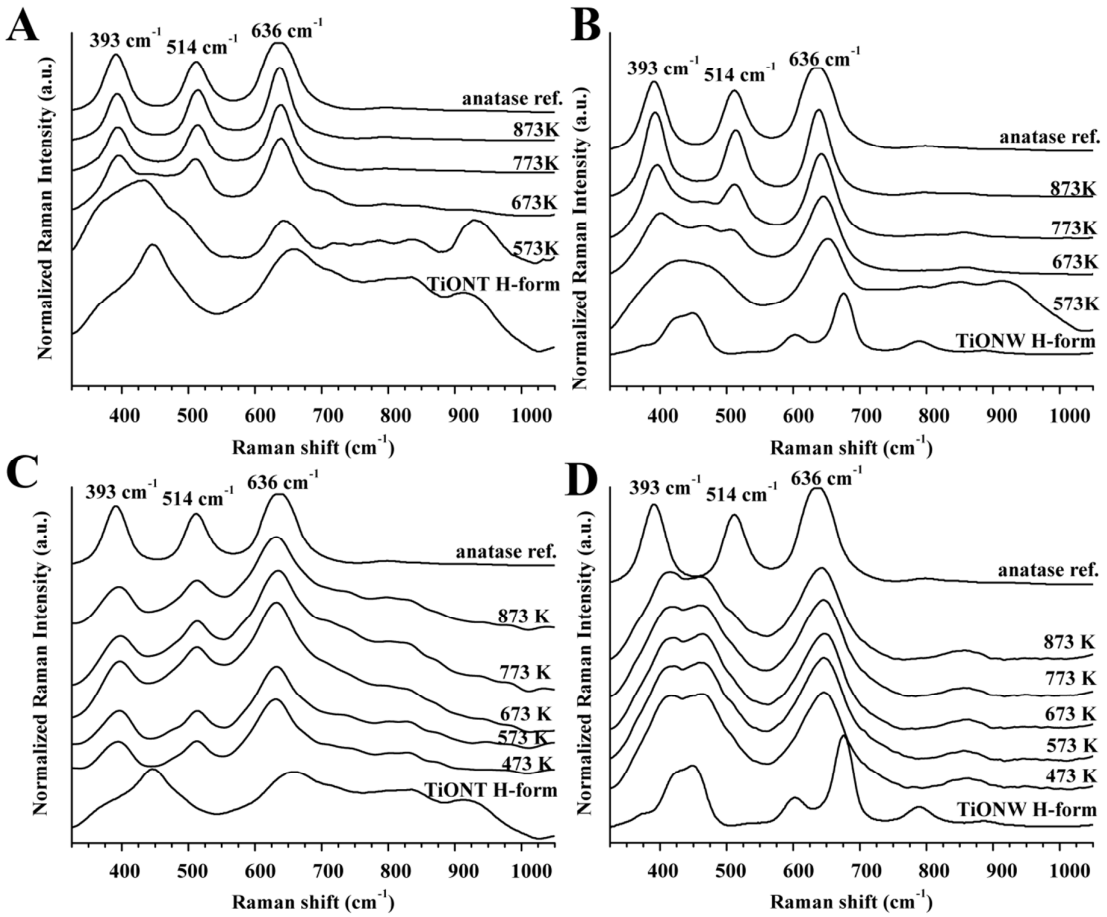

Fig. 4. Normalized Raman spectra of the thermal behavior of H-form titanate nanotubes (A) and nanowires (B). Graphs C and D illustrate the thermal behavior of Au loaded titanate nanotubes and wires, respectively. The commercial anatase reference sample is shown at the top of each spectra.

Figure 5

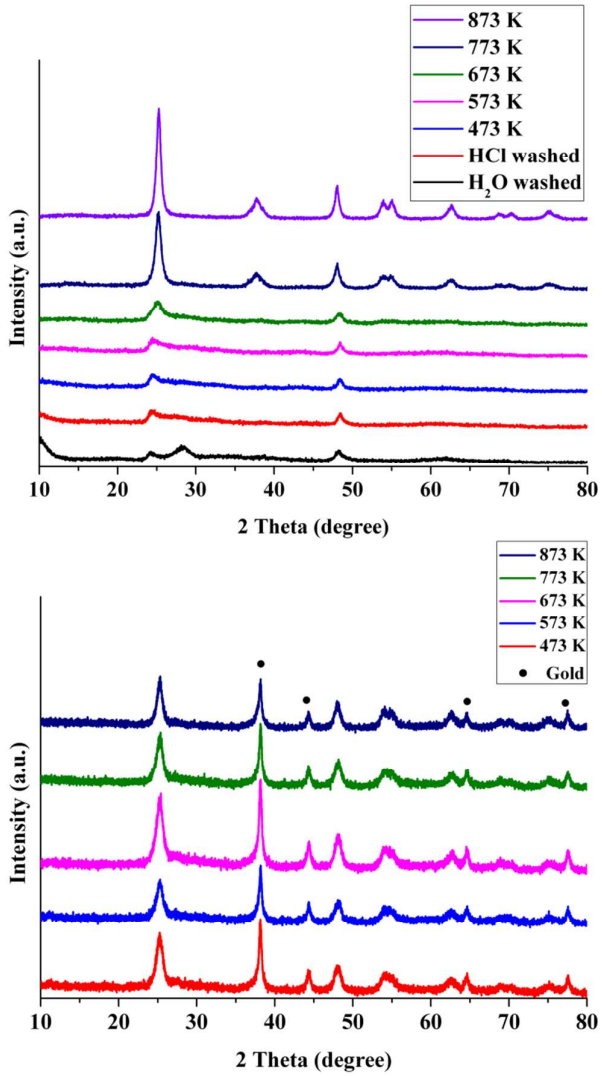

Fig. 5. XRD of H_2O washed and H-form titanate nanotubes (upper part) and Au loaded (2.5%) nanotubes (lower part) as a function of annealing temperature.

Figure 6

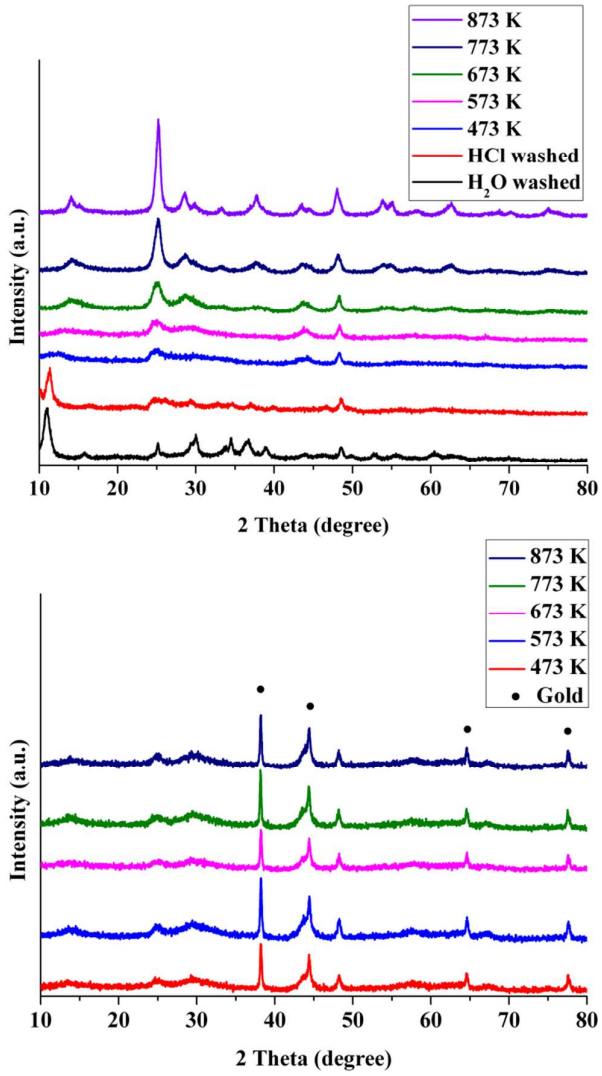

Fig. 6. XRD of H_2O washed and H-form titanate nanowires (upper part) and Au loaded (2.5%) nanowires (lower part) as a function of annealing temperature.

Figure 7

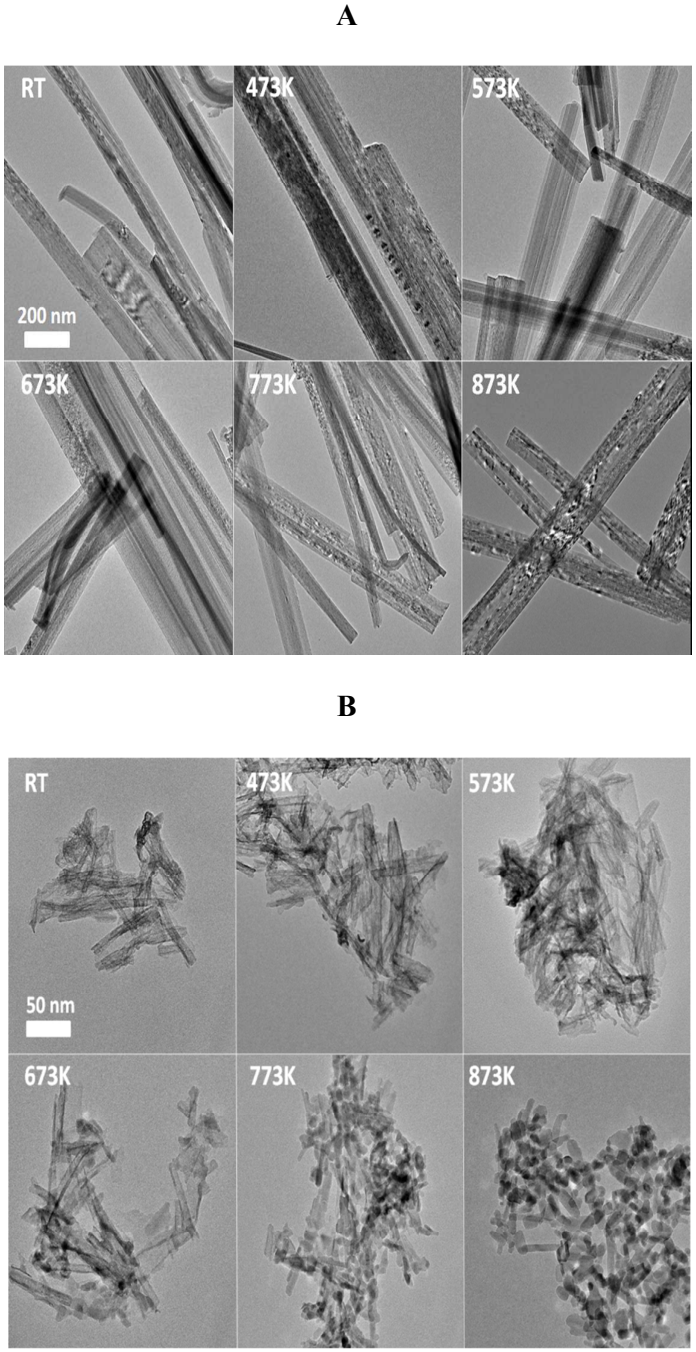

Fig. 7 TEM images of H-form nanotubes (A) and H-form nanowires (B) at different temperatures.

Figure 8

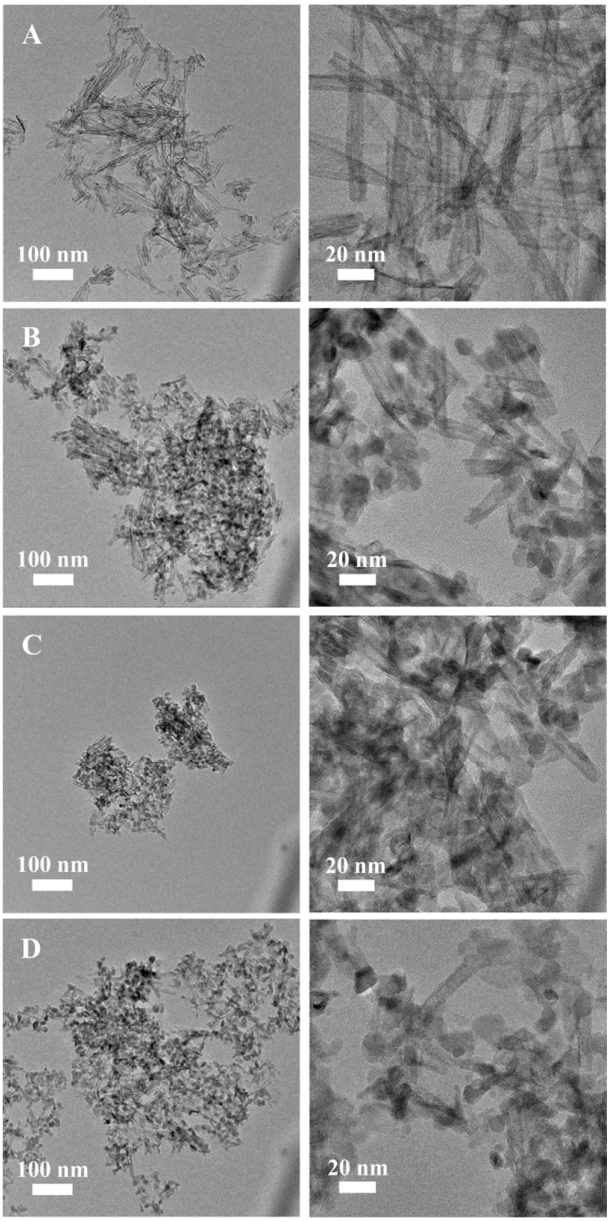

Fig. 8. HRTEM images of H-form titanate nanotubes (A) and Au containing (2.5 %) nanotubes after different heat treatments; B – 473 K, C – 673 K, D – 873 K.

Figure 9

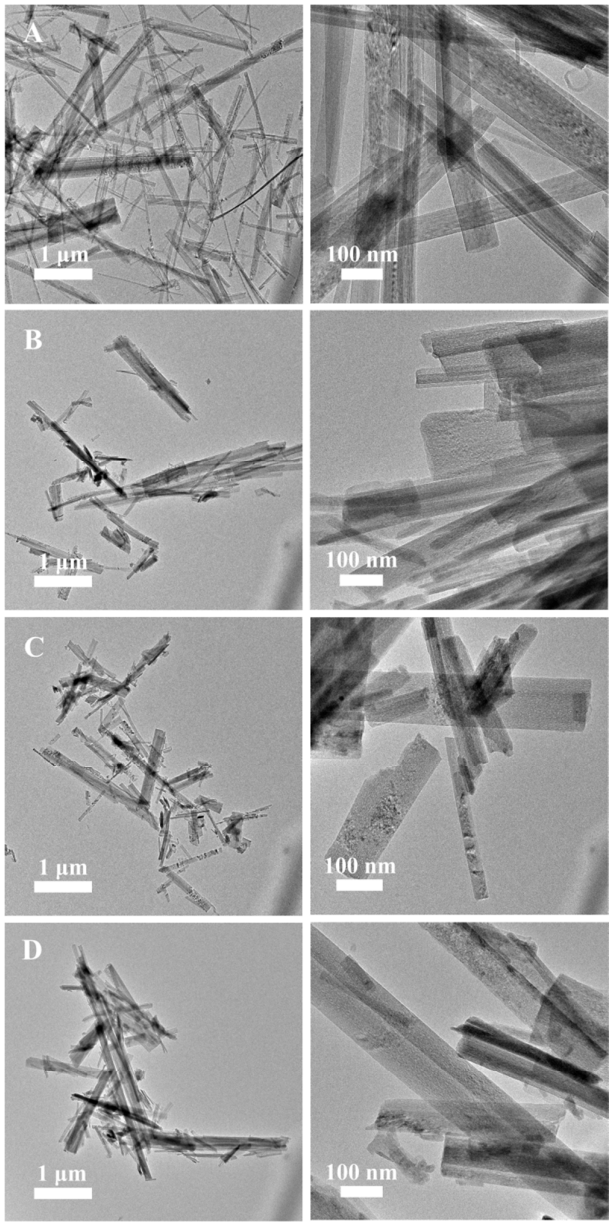

Fig. 9. HRTEM images of H-form titanate nanowires (A) and Au containing (2.5 %) nanowires after different heat treatments; B – 473 K, C – 673 K, D – 873 K.

Figure 10

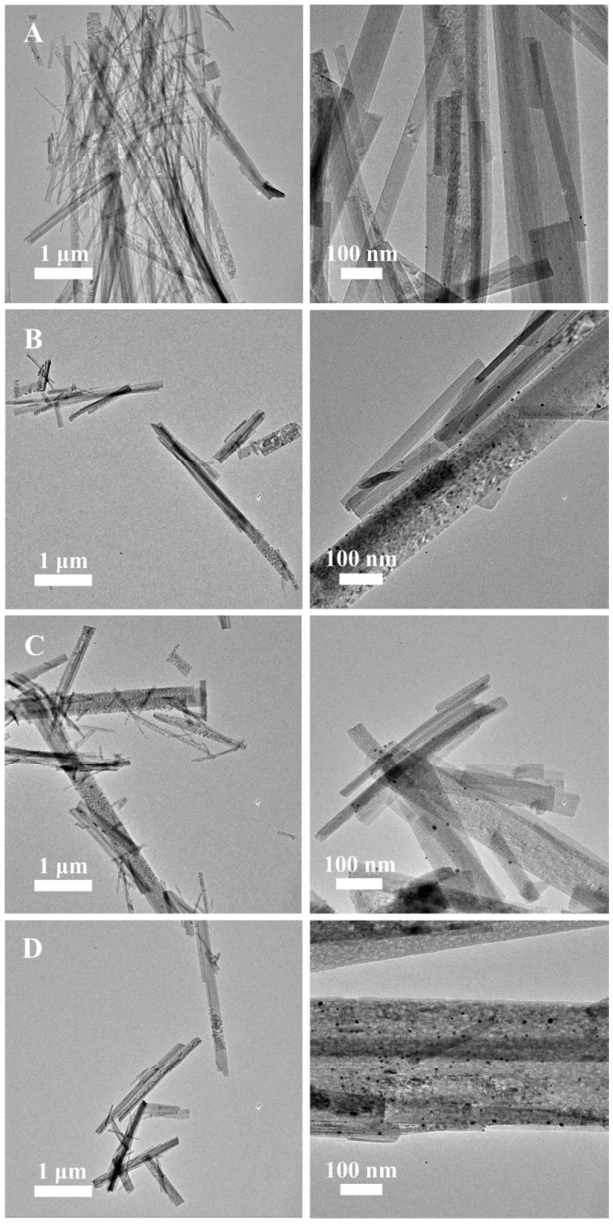

Fig. 10. HRTEM images of Au containing (2.5 %) nanowires (obtained by $NaBH_4$ reduction). H-form titanate nanowires (A) and after different heat treatments; B – 473 K, C – 673 K, D – 873 K.

DEPARTMENT OF PHYSICAL CHEMISTRY AND MATERALS SCIENCE
MTA-SZTE REACTION KINETICS AND SURFACE CHEMISTRY RESEARCH GROUP OF THE HUNGARIAN ACADEMY OF SCIENCES

Prof. Dr. János Kiss
UNIVERSITY OF SZEGED
6701 Szeged, Aradi v square 1.
Hungary

Address: P. O. Box 168. Tel.: 36-62-544-803 Fax: 36-62-544-106 E-mail: jkiss@chem.u-szeged.hu
http:www.staff.u-szeged.hu/~jkiss/

Sept. 05, 2014

Dr. Anna Simpson

Editor

Physical Chemistry Chemical Physics

Dear Dr Simpson,

Enclosed please find our manuscript entitled „ **Influence of Gold Additive on the Stability and Phase Transformation of Titanate Nanostructures"** which is submitting for publication in Physical Chemistry Chemical Physics. We hope that our manuscript matches well in your profile.

This present paper is a continuation of our previous works, where we studied the formation, characterization of nanosized metal particles on titanate nanowires and nanotubes and their effects on stability and phase transformation of titanate nanostructures. See examples: **"Metal loading determines the stabilization pathway for Co^{2+} in titanate nanowires: ion exchange vs. cluster formation"** paper was published in PCCP (2013, **15,** 15917-15925) and "**Rh-induced Support Transformation Phenomena in Titanate Nanowire and Nanotube Catalysts"** was published in Langmuir (2013, **29,** 3061-3072).

I am the corresponding author. The submission and revision process will be handled by me (email: jkiss@chem.u-szeged.hu). In case of any questions please don't hesitate to contact me.

Best regards

Prof. János Kiss